Rothamsted Repository Download

A - Papers appearing in refereed journals
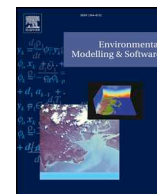
The publisher's version can be accessed at:

- https://dx.doi.org/10.1016/j.envsoft.2019.05.005

The output can be accessed at: https://repository.rothamsted.ac.uk/item/8wwwx.

© 8 May 2019, Please contact library@rothamsted.ac.uk for copyright queries.

New modelling technique for improving crop model performance - Application to the GLAM model

I. Droutsas[a,b,*], A.J. Challinor[a,b,c], M. Swiderski[a], M.A. Semenov[d]

[a] *Institute for Climate and Atmospheric Science, School of Earth and Environment, University of Leeds, LS2 9JT, Leeds, UK*
[b] *Priestley International Centre for Climate, University of Leeds, LS2 9JT, Leeds, UK*
[c] *Collaborative Research Program from CGIAR and Future Earth on Climate Change, Agriculture and Food Security (CCAFS), International Centre for Tropical Agriculture (CIAT), A.A. 6713, Cali, Colombia*
[d] *Rothamsted Research, Harpenden, Herts, AL5 2JQ, UK*

ARTICLE INFO

ABSTRACT

Crop models simulate growth and development and they are often used for climate change applications. However, they have a variable skill in the simulation of crop responses to extreme climatic events. Here, we present a new dynamic crop modelling method for simulating the impact of abiotic stresses. The Simultaneous Equation Modelling for Annual Crops (SEMAC) uses simultaneous solution of the model equations to ensure internal model consistency within daily time steps; something that is not always guaranteed in the usual sequential method. The SEMAC approach is implemented in GLAM, resulting in a new model version (GLAM-Parti). The new model shows a clear improvement in skill under water stress conditions and it successfully simulates the acceleration of leaf senescence in response to drought. We conclude that SEMAC is a promising crop modelling technique that might be applied to a range of models.

1. Introduction

The plant growth and development are influenced by a wide range of biotic and abiotic factors. Understanding the complex interactions between plants and their surrounding environments is important for prediction under environmental change. In this context, crop models are developed as systems for describing the growth and development of a crop in any given environment at local, regional or even global scale (Chenu et al., 2017). Crop models simulate the plant growth and development by using a set of mathematical equations and they often include complex functions and modelling techniques for their simulations (Marcelis et al., 1998). They are widely used as agricultural tools to describe the plant performance and to predict the final production and yield.

Climate change brings a higher frequency of extreme weather events and more complex interactions which can damage the crops, limit their yield (Howden et al., 2007; Porter et al., 2014; Zhao et al., 2017), and alter their nutritional properties (Myers et al., 2014; Jones et al., 2017). Crop modelling has a long history in simulating these complex interactions. However significant challenges remain if the risks posed by climate change are to be reliably quantified (Challinor et al., 2014). Extreme events, and the abiotic stresses that result, are

particularly challenging, especially considering the wide range of environments across which crops are cultivated. The simulation of crop performance in these extreme climatic conditions can be significantly uncertain (Zhang and Tao, 2013; Asseng et al., 2013, 2015). Tao et al. (2018) showed that for climate change impact assessment, the largest source of uncertainty in their crop model ensemble was due to the model structure. Rivington and Koo (2010) suggests that one of the ways to improve the crop model performance is by better simulating the various processes through an improved connection between them. Thus, improving the crop model structure is a significant step towards reducing the uncertainty in the model output for climate change impact studies (Challinor et al., 2013).

A common practice to improve the performance of a crop model is to add new processes and interactions (Affholder et al., 2012). It is expected that this practice will lead to an improvement in skill, while at the same time the model will be able to simulate more processes of the real world. Nevertheless, adding complexity in a crop model may not always lead to an improvement in skill, especially in large scale applications. This can partially occur from the inclusion of site-specific parameters and processes that are difficult to generalize in larger regions (Challinor et al., 2009). This is a common problem in crop modelling and in some cases modellers tend to develop simplified
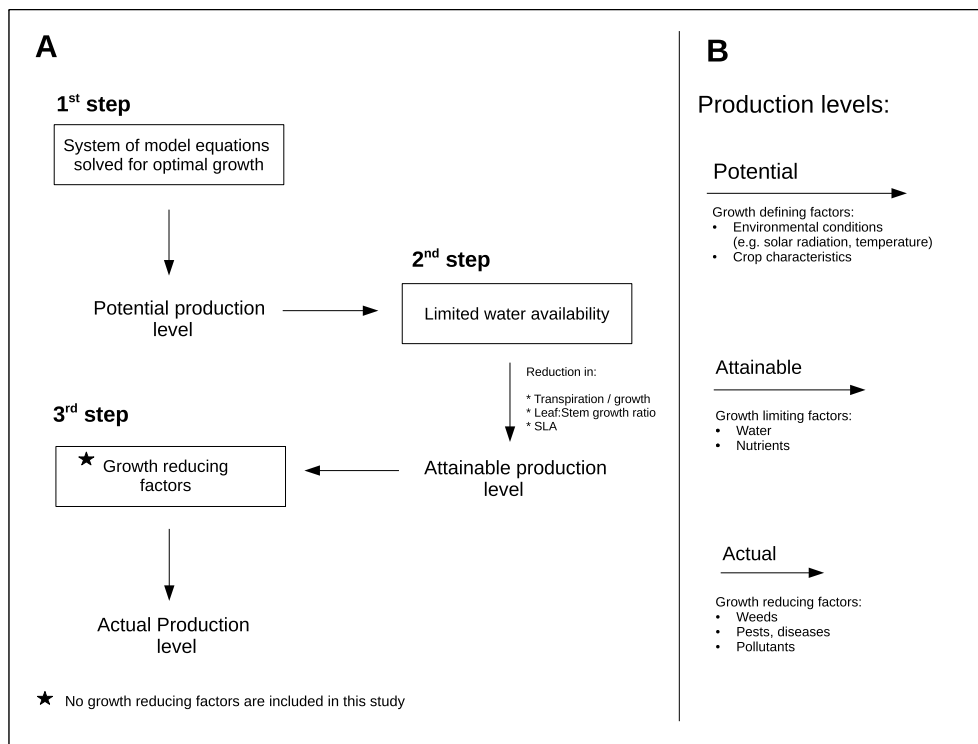
Fig. 1. A. SEMAC methodology for crop production; B. Production levels in Wageningen crop models (Van Ittersum and Rabbinge, 1997; van Ittersum et al., 2003).

versions of models that are already very complex (e.g., Stella et al., 2014). According to Passioura (1996) there is an optimal level of complexity in which the total model error is minimized. At this point, there is a balance between a robust model structure and the number of parameters included. In accordance with that, crop modellers should design their models upon an appropriate level of complexity (Sinclair and Seligman, 2000). This level is defined by the scope of the model and the scientific questions that it seeks to address (Challinor et al., 2018).

Simultaneous equation modelling approaches are commonly used to provide a robust way of simulating the interdependence between processes that are jointly determined in the real world (e.g., Oldroyd, 1950; Chou and Kamel, 1988; Zeng and Cai, 2005; Lefcheck, 2016). Agricultural environments consist of complex systems with many interactions and the interdependence between various processes makes modelling difficult. The aim of this paper is to introduce a new crop modelling method which uses simultaneous solution of all model equations for crop growth and development. The new approach is called SEMAC (Simultaneous Equations Modelling for Annual Crops). The solution of the system of equations returns the values of the state variables for growth and development of the crop. This is done twice for each time step, initially for optimal conditions, where the impact of any stresses is ignored, and then again after considering of the environmental limitations. Applying the new modelling technique results in a dynamic crop model with reduced parameterization requirements, robust structure, and improved internal consistency.

SEMAC is implemented here in the GLAM crop model and a new model version is formed. The new model is called GLAM-Parti as it introduces partitioning of biomass based on allometric relationships; a necessary step for the application of SEMAC. GLAM-Parti advantages over GLAM since it has improved model structure, it gives a better connection between the model processes and finally, it increases the ability of the model to capture the impact of water stress on crop growth and development.

2. Rationale and methodology

2.1. Methodology and internal consistency in SEMAC

The simultaneous solution of model equations is not a new concept in crop modelling. For instance, simultaneous modelling approaches have been developed to couple leaf photosynthesis to stomatal conductance (e.g., Baldocchi, 1994; Yin and Struik, 2009). In addition, Goudriaan and Van Laar (1994) combined the rate of formation of new leaf area and the growth of biomass to develop an equation which explains the evolution of the total biomass during the season. Nevertheless, in order to avoid a very complicated system, they made simplifications, such as that the relative growth rates of biomass and leaf area are identical and constant over time.

SEMAC develops a system of simultaneous equations which accounts for all above-ground crop growth and development processes. This differentiates SEMAC from the prevailing crop modelling techniques. Otherwise, the modelling process follows the methodology described in van Ittersum et al. (2003). At the first step (i.e. the potential production level) the crop growth is defined by the given environmental conditions and the crop properties without considering of any limitations from stresses. At this step, the system of equations is solved to return the potential crop production level. At the second step (i.e. the attainable production level) the impact of stresses is taken into account - in this case water stress - which reduces transpiration and growth, decreases the specific leaf area (SLA), and alters the allocation of dry matter between leaves and stems. These modifications are incorporated into the model equations, which are solved to return the values of the state variables of the system and it outputs the attainable production level. At the third step, the growth reducing factors are taken into account (i.e. weeds, pests, diseases, pollutants). In SEMAC, the steps 1–3 are always carried out in order as necessary (Fig. 1).

Applying SEMAC to a crop model involves the following steps:

i) Introduction of allometric relationships to relate state variables:

There are various modelling techniques for simulating the carbon allocation among the plant organs. Common approaches are the use of partitioning coefficients that are dependent on the development stage or modelling the source to sink carbon dynamics (Marcelis and Heuvelink, 2007). In SEMAC, the concept of allometric growth is implemented, which expands upon the principle that the growth of the different plant compartments is jointly determined through allometric relationships. Based on these relationships, the total biomass (W) can be expressed as function of LAI, following the modifications shown in Section 3.4.2.

ii) Expression of any remaining state variables as functions of other state variables: In crop models, the daily increase in biomass (dW/dt) is estimated either from intercepted radiation, transpiration or photosynthesis. At the canopy level, the biomass growth can be expressed as function of LAI (i.e. this is especially true for radiation or transpiration driven models). For instance, in water-based crop models, the production of new biomass depends on canopy transpiration. The transpiration is a function of evapotranspiration, which is in turn dependent on the environmental conditions and LAI. After calculating the environmental influence (i.e. based on the weather conditions), the growth of biomass can be expressed as function of LAI (see Section 3.4.3 and Appendix A).

iii) Substitution of the relationships from i and ii into the simple mass balance equation $W_n - W_{n-1} - dW/dt = 0$. The W_n and dW/dt terms of the equation are explained in steps i, ii, where they are expressed as function of LAI. W_{n-1} is the biomass value of the previous time step. The solution of the mass balance equation returns the value of LAI which is then used to solve all other equations that participate into the system. This is done twice, initially for optimal conditions, where the stress impact is ignored, and then again, after incorporating the stress effects. In this study water stress is considered, however SEMAC can be similarly applied to various stress conditions. A schematic representation of the implementation of SEMAC in crop models is given in Fig. 2.

2.2. Use of SEMAC to model stress conditions

The implementation of SEMAC leads to three main potential sources of error in the simulation of crop growth and development at each time step. These are: the production of new biomass, the allocation of biomass to the differ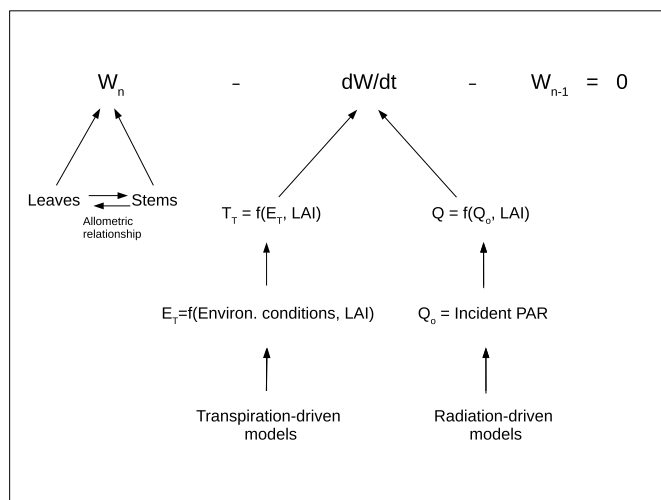ent plant compartments and the canopy SLA. The first two aspects affect the accuracy of the model to simulate the above-ground biomass and the masses of the different organs (e.g. leaves, stems, grains). The third aspect (i.e. the SLA) affects both the simulation of leaf mass and the estimation of LAI. This accounts for all climatic conditions and abiotic stresses. More specifically, various stresses and management practices can significantly affect the plant growth (Cramer et al., 2011) and alter the dry matter allocation patterns (Weiner, 2004; Sieling et al., 2016; Poorter et al., 2012). In crop models, the biomass accumulation rate may be modified and the SLA as well as the carbon partitioning between different organs may be adjusted to the environmental conditions (i.e. through modifications in the allometric relationships). SEMAC provides a simple modelling framework for simulating these growth and development processes and ensures internal model consistency with the use of the simultaneous equation modelling. This secures that there are no missing interactions between processes that are interconnected in the field, which is particularly important under stress conditions where the system becomes more complex. Crop modelling techniques based on sequential approaches may face issues in capturing the plant/environment interactions at the same time step.

2.3. Modelling water stress effects in SEMAC

Most crop models use a water stress factor to simulate the impact of water shortage on crops (e.g., Jamieson et al., 1998; Asseng et al., 2004). This factor is usually calculated as the rate of the available water in the soil to the total water demand by the plant. If this rate is below a pre-determined threshold then the plant is affected by the water deficit. The water stress factor takes values from zero to one and it is usually applied to modify LAI or accelerate leaf senescence (Raes et al., 2009; Ewert et al., 2015).

Nevertheless, the leaf development is affected by various factors under limited water in the field. Most importantly, drought conditions may alter the leaf:stem mass ratio (Ratjen et al., 2016) and decrease the SLA (Fernández and Reynolds, 2000; Brisson and Casals, 2005; Zhang et al., 2010). If these effects are omitted in a crop model, a bias may be introduced in the simulation of leaf dynamics (Ratjen et al., 2016). For this reason, in SEMAC, LAI is not directly effected by the water stress effects. Instead, the water stress factor is used to apply modifications on the leaf:stem dry matter production and the canopy SLA under drought. LAI is then altered both due to decreased carbon allocation to the leaves and to lower SLA. Simultaneously, the biomass production is affected by the LAI reduction. These effects are captured at the same time step due to the robust model structure and the simultaneous solution of the model equations. Through this method, both the LAI takes into account the water stress effects on leaf growth and development, and all state variables (including biomass growth) are consistent with the value of LAI, since they are updated by the same system of equations.

2.4. Modelling of stress interactions

Climate change brings a higher frequency of extreme weather conditions and more stress interactions acting on crops (Gray and Brady, 2016). When multiple stresses affect the crop performance, the response of plants cannot be addressed only by taking into account of each stress individually (Mittler, 2006). In crop modelling studies, the simulation of crop growth and development in these environments can be very complex. For instance, in drought prone regions with high air pollution levels, the use of multiple factors to simulate the leaf expansion or accelerate leaf senescence may result to an unrealistic model output. SEMAC attempts to increase the model predictability in these situations by introducing an improved connection between the various model processes. LAI is computed by the system of equations which decreases the parameterization requirements, as it removes the need of using stress factors to modify the LAI growth. It also improves the LAI simulation since it takes into account all equations in the system for the estimation of LAI. The use of allometric relationships for the

Fig. 2. Implementation of SEMAC in radiation and transpiration driven crop models. T_T = Transpiration, E^T = Evapotranspiration, Q = Intercepted PAR, W = total above-ground biomass, dW/dt = daily increase in biomass, n = time step. W_n and dW/dt are expressed as function of LAI and the solution of the mass balance equation returns the value of LAI.
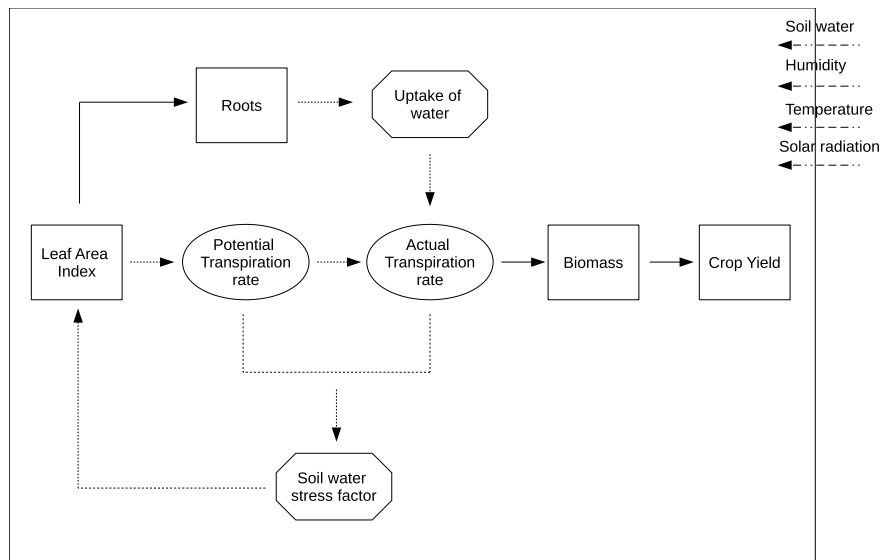
Fig. 3. Generic scheme of GLAM model. The categorization of variables is taken from Loomis et al. (1979). State variables are represented by boxes, rate variables by ellipses, auxiliary variables by octagons, external variables by 2 dots - 3 dashes lines. Mass flows are represented by solid-line arrows, information flows by dashed-line arrows.

partitioning of biomass gives the opportunity to easily shift the carbon allocation between the plant compartments under different environmental conditions. The above advancements create a modelling framework which can be further expanded to incorporate more stresses. Hence, it is believed that SEMAC can be a useful tool in the attempt to address the crop response to a changing climate.

3. Materials and methods

3.1. GLAM model

The General Large Area Model for annual crops (GLAM) is a process – based crop model which simulates the impact of climate on crop yield (Challinor et al., 2004) (Fig. 3). It is a relatively simple model which runs in daily time step and it is designed to operate at regional scales (Challinor et al., 2005). GLAM uses a maximum daily growth rate of leaf area index which can be decreased by the water stress. The daily potential evapotranspiration is calculated by the Pristley-Taylor equation and it is partitioned into potential evaporation and potential transpiration. The actual transpiration is calculated from the potential transpiration by taking into account the soil water content. The transpiration is multiplied by the transpiration efficiency to return the daily biomass growth. The grain yield is estimated by partitioning the aboveground biomass to the grains using the harvest index. Challinor et al. (2004) provides a detailed description of GLAM.

In GLAM, the grain growth is dependent on canopy transpiration. However, under drought conditions, either the photosynthesis or the remobilization of pre-anthesis assimilates to the grains play a major role on grain yield (Inoue et al., 2004). In order to capture this effect, the radiation use efficiency (RUE) approach – i.e. the second option for simulating growth in GLAM (Osborne et al., 2013) - was selected to describe the increase in biomass, only after anthesis when extremely low values of canopy transpiration were calculated. A threshold for transpiration was set below which the RUE approach was used. Severe drought effects have been previously reported to occur for wheat at anthesis in 80% of water deficit (Mahrookashani et al., 2017). In accordance to that, the model threshold was set to the 0.2 value of the soil water stress factor.

3.2. Internal consistency in GLAM

GLAM uses a sequential method for solving the model equations at each time step. This can limit the model performance in the simulation of processes that interact in the field. Fig. 3 is a schematic representation of the GLAM model structure. LAI is initially estimated and the potential canopy transpiration is calculated according to the LAI value. The actual transpiration is a fraction of the potential value based on the soil water content. Under water stress, the actual transpiration is reduced due to the soil water deficit. The decreased transpiration rate reduces the production of new biomass. In such case, the growth of leaves should also be lower due to the water stress effects. However, LAI is already calculated in the model and it is used for the calculation of the other state variables. Therefore, LAI does not respond dynamically to water stress. For this reason, the soil water stress factor is computed which reduces the growth of leaves on the next time step (i.e. the next day). This is a form of inconsistency, since this time delay is not representative of the reality and limits the model skill in the simulation of the drought stress effects.

3.3. GLAM-Parti development

GLAM-Parti is the new version of GLAM based on the SEMAC approach (Fig. 4). The model modifications are described in Section 3.4. The alterations start with the inclusion of an allometric relationship between leaves and stems and expand with the incorporation of the new methodology. The value of LAI and the masses of leaves, stems and the total above-ground biomass are extracted simultaneously and there is no time lag between them, something that may occur in the step-by-step modelling method (e.g. the LAI value of the previous day is used for the computation of the carbon assimilation on the next day).

In GLAM-Parti, the set of model equations is initially solved to calculate the maximum plant growth at daily time step. This growth rate corresponds to the level defined only by temperature, radiation, vapour pressure deficit (VPD) and the plant properties (e.g. transpiration efficiency). Next, the available soil water is estimated. Based on the level of the water in the soil, the actual transpiration and the water stress factor are calculated. The actual transpiration is used to compute the growth of the above-ground biomass. The water stress factor is used to alter the SLA and the allocation of dry matter between leaves and stems. These modifications are incorporated into the set of model equations which is solved again to return the values of all growth variables and the attainable production level. The yield gap parameter (YGP) is used to estimate the actual production level for all growth-reducing factors that the model implicitly takes into account. In this study, water stress is the only yield limiting factor, thus no growth reducing factors are considered.

The incorporation of the SEMAC methodology into GLAM simplifies the modelling of canopy LAI and leads to reduced parameterization
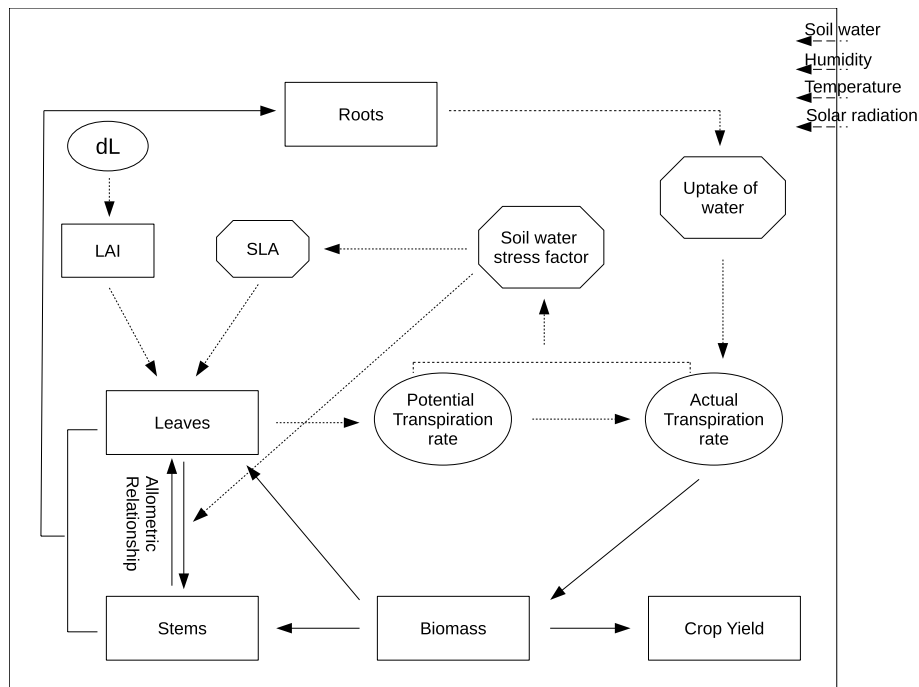
Fig. 4. GLAM-Parti model structure. The system of equations is solved numerically by iteration with the Newton-Raphon approach. The unknown variable is dL (leaf area change). The iteration process stops when the system converges. The categorization of variables is taken from Loomis et al. (1979). State variables are represented by boxes, rate variables by ellipses, auxiliary variables by octagons, external variables by 2 dots - 3 dashes lines. Mass flows are represented by solid-line arrows, information flows by dashed-line arrows.
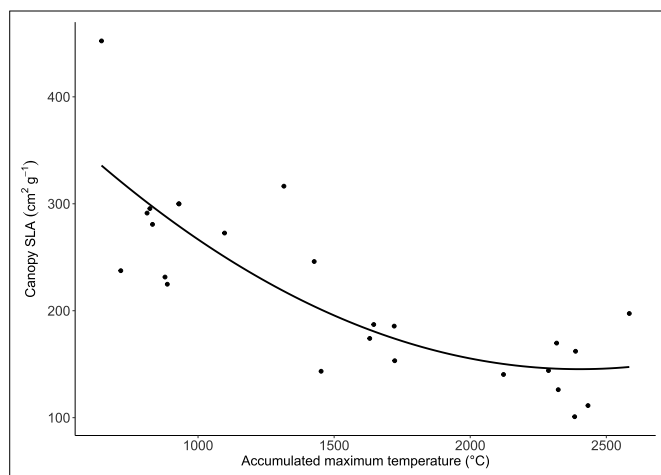

Fig. 5. Quadratic regression between canopy SLA and the accumulated maximum temperature index. Continuous line is the regression: $y = 501 - 0.296x + 6.17 \cdot 10^{-5} x^2$ ($R^2 = 0.68$, $p < 0.01$).

requirements. The maximum LAI expansion rate $(dL/dt)_{max}$ is removed, which is a parameter used for the calculation of LAI. The model has been previously seen to be particularly sensitive to this parameter value (Ramirez-Villegas et al., 2017) and its removal decreases the model error significantly (i.e. in the results, GLAM-Parti improves upon GLAM in all LAI simulations).

In this study, SEMAC stops at anthesis since at the post-anthesis period the model runs with a combination of the transpiration and the radiation use efficiency methods. This step is currently not included in GLAM-Parti, however the model is under ongoing development. At plant maturity, all leaf area is simulated to be senescent, therefore at the end of the grain-filling period if there was still green leaf area, the LAI is set to zero.

3.4. GLAM modifications

3.4.1. Leaf dynamics

In crop modelling studies, SLA is used for the simulation of the leaf

dynamics. Generally, it is set either as an input parameter (Yin and Struik, 2010) or it is defined as a function of plant age, growth stage or the environmental conditions (Hoogenboom et al., 1992; Marcelis et al., 1998; Asseng et al., 2003; Leutscher and Vogelezang, 1990). In GLAM, biomass and leaf area are simulated separately and SLA is permitted to evolve, subject to constraints based on an observed maximum value. This approach is inconsistent with SEMAC, since it does not result in full partitioning of biomass. In GLAM-Parti we make use of a significant observed relationship between SLA and temperature in various plant species (Loveys et al., 2002; Rosbakh et al., 2015; Atkin et al., 2005). For wheat too, SLA has been previously seen to be sensitive to temperature variations (Hotsonyame and Hunt, 1998).

For the parameterization of SLA, data analysis was conducted on the "Hot Serial Cereal" experiment (Martre et al., 2018). Wheat was grown in different periods of the year and the impact of temperature on growth and development was examined. Here, we tested the impact of high temperature on the evolution of the canopy SLA over time. We accumulated all daily maximum temperatures for the period from leaf emergence to the day of leaf measurement and compared them to the observed SLA as follows: SLA was calculated as the reciprocal of the measured specific leaf weight (SLW) and the data points with a coefficient of variation greater than 0.3 (i.e. 30%) were excluded (Taylor et al., 1999) (there was only one such point with value 0.49). A significant relationship was observed between the SLA and the accumulated maximum temperature index (T_{mac}) (Fig. 5). A quadratic model was selected to best fit the relationship:

$$SLA = 501 - 0.296 \cdot Tmac + 6.17 \cdot 10^{-5} \cdot Tmac^2 \tag{1}$$

where,

$$T_{mac} = \sum_{i=IEM}^{n} T_{max_i} \tag{2}$$

T_{max} is the daily maximum temperature, IEM is the day of crop emergence and n is the number of days after crop emergence. Eq. (1) describes canopy SLA as a function of the maximum temperature events accumulated over the crop growing season.

3.4.2. Partitioning of biomass between leaves and stems

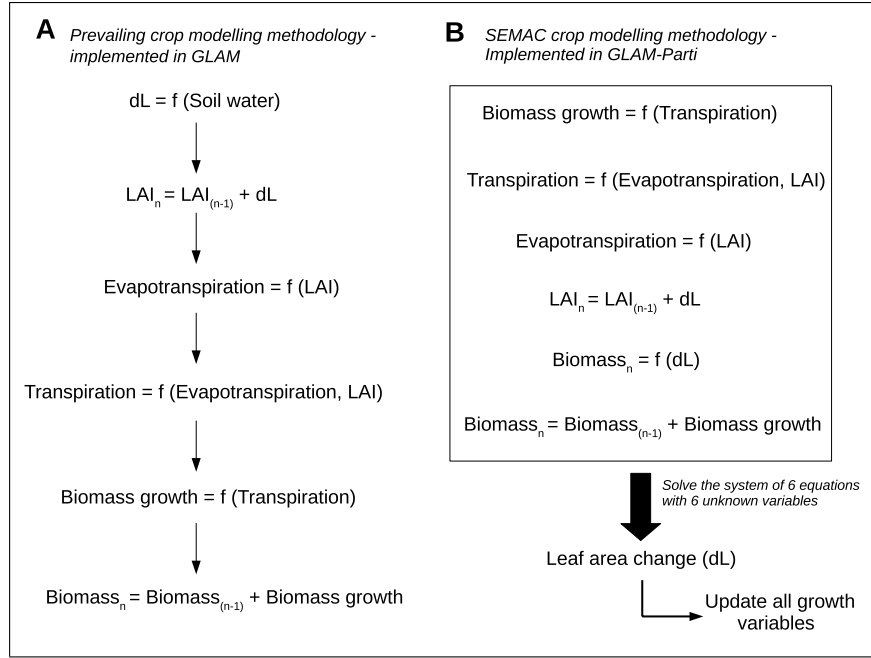In GLAM, LAI is the first state variable to be updated in the model

Fig. 6. A. Well-established crop modelling methodology implemented in GLAM; B. SEMAC methodology for crop growth and development.

based on a prescribed maximum LAI growth, which can be reduced only by limited soil water. For the incorporation of SEMAC, the function of LAI growth was removed. Instead, an allometric relationship was introduced which describes the partitioning of biomass between leaves and stems. According to the allometric approach the mass of stems (M_S) can be described in relation to the mass of leaves (M_L) under the generic formula (Enquist et al., 1998; Poorter et al., 2012):

$$M_S = h \cdot M_L^g \tag{3}$$

where g, h are empirically determined parameters and their values for wheat are taken from Ratjen et al. (2016) (i.e. the parameter h of this study is equal to the e^h of Ratjen et al. (2016)). The total mass of leaves (M_L) is divided into green leaves (M_{GL}) and yellow leaves (M_{YL}):

$$M_L = M_{GL} + M_{YL}$$
$$= \frac{LAI}{SLA} + M_{YL} \tag{4}$$

The above-ground biomass (W) is divided into stems, leaves and grains. For the period before the initiation of grain development, W can be described by Eqs. (3) and (4) as:

$$W = M_L + M_S$$
$$= \frac{LAI}{SLA} + M_{YL} + h \cdot \left(\frac{LAI}{SLA} + M_{YL} \right)^g \tag{5}$$

3.4.3. Incorporation of SEMAC into GLAM

Eqs. (3)–(5) are newly imported equations in GLAM. These are combined with the existing functions to form GLAM-Parti as follows:

In GLAM, the potential evapotranspiration ($E_{pot}T$) is calculated by the Priestley-Taylor equation as:

$$E_{pot}^T = \frac{\alpha}{\lambda} \cdot \frac{\Delta(R_N - G)}{\Delta + \gamma} \tag{6}$$

and it is partitioned to potential evaporation and transpiration, out of which the potential transpiration (T_T) is calculated as:

$$T_T = E_{pot}^T (1 - e^{-kLAI}) \tag{7}$$

The growth of the above-ground biomass (dW/dt) is defined as:

$$\frac{dW}{dt} = T_T \cdot TE \tag{8}$$

where TE is the transpiration efficiency and it is calculated as:

$$TE = min\left(\frac{E_T}{V}, E_{TN,max} \right)$$

E_T is the normalised transpiration efficiency in Pa, V is the vapour pressure deficit, and $E_{TN,max}$ is the maximum transpiration efficiency in g kg^{-1}. LAI can be expanded as:

$$LAI_n = LAI_{n-1} + dL \tag{9}$$

where LAI_n is the value of LAI at any given n day, LAI_{n-1} is the LAI of the previous day and dL is the leaf area change between the two consecutive days. Finally, the above-ground biomass of the n day (W_n) is equal to the biomass of the previous day (W_{n-1}) plus the growth in biomass between the two days (dW/dt), which makes:

$$W_n - \frac{dW}{dt} - W_{n-1} = 0 \tag{10}$$

Eqs. (5)–(10) form a system of 6 equations with 6 unknown variables which can be solved simultaneously to return the values of each unknown variable (i.e. dL, LAI_n, $E_{pot}T$, T_T, dW/dt, W_n). For the solution of the system, Eqs. (5)–(9) are substituted into Eq. (10) which gives:

$$\underbrace{\frac{LAI_{n-1} + dL}{SLA} + M_{YL} + h \cdot \left(\frac{LAI_{n-1} + dL}{SLA} + M_{YL} \right)^g}_{W_n} -$$
$$\underbrace{\frac{TE \cdot \alpha \cdot \Delta \cdot R_N}{\lambda \cdot (\Delta + \gamma)} (1 - C_G \cdot e^{-k(LAI_{n-1} + dL)})(1 - e^{-k(LAI_{n-1} + dL)})}_{dW/dt} - W_{n-1} = 0 \tag{11}$$

Eq. (11) forms the core of the SEMAC methodology (Fig. 6) and it is a function of leaf area change (dL). It can be solved numerically by iteration with the use of the Newton-Raphson method. The iteration process ends when the difference in the value between two consecutive loops is < 0.01. The extracted value of dL is used to update the variables in Eqs. (3)–(9). Detailed description of the derivation of the dW/dt term in Eq. (11) is provided in Appendix A. Whenever a negative value of dL is calculated, M_{YL} is updated as:

$$M_{YL(n)} = M_{YL(n-1)} + \frac{|dL|}{SLA} \tag{12}$$

where $M_{YL(n)}$ is the mass of yellow leaves on the n day, and $M_{YL(n-1)}$ is the mass of yellow leaves on the previous day (n-1). Eqs. (3)–(11) form

the 1st step of SEMAC in which no stress affects the crop growth and development (i.e. the potential production level).

3.4.4. Root modelling in GLAM-Parti

In GLAM the roots grow under a prescribed extraction front velocity and a prescribed root length density at the extraction front. The root length density by volume is calculated as a function of LAI and is used for the computation of the potentially extractable soil water (Challinor et al., 2004). In GLAM-Parti, the modelling of root growth is modified. A root partitioning coefficient (R_c) is introduced which describes the increase in root biomass (dW_R) as a fraction of the total biomass increase (dW_T). The roots grow from plant emergence to anthesis and R_c is defined as:

$$R_C = \frac{dW_R}{dW_{AG} + dW_R} \tag{13}$$

Where dW_T is divided into above-ground (dW_{AG}) and root biomass growth (dW_R). The solution of Eq. (13) for dW_R gives:

$$dW_R = \left(\frac{R_C}{1 - R_C}\right) \cdot dW_{AG} \tag{14}$$

The computation of R_c is taken from Baret et al. (1992) and it is a function of the growth degree days (GDD) after sowing normalised at spiking:

$$R_C = -0.15 + 0.63 \cdot e^{-0.98 \cdot \theta^*} \tag{15}$$

where,

$$\theta^* = \frac{\theta - \theta_e}{\theta_s - \theta_e} \tag{16}$$

θ is the GDD after sowing, θ_e and θ_s are the GDD from sowing to emergence and from sowing to spiking (i.e. 150 GDD before anthesis) accordingly.

The root biomass is daily updated based on the allometric relationship of Eq. (14) to form the total root biomass (W_R). The W_R is divided by the specific root weight (σ) to give the total root length (R_L). The value of σ for wheat is assumed to be constant at 4.57 g km^{-1} (King et al., 2003). The soil is divided into 25 layers (NSL = 25), each with 10 cm thickness (DZ = 10). The root length density of each soil layer (L_{VSLi}) is estimated according to the modelling method of King et al. (2003):

$$L_{VSLi} = (Y_{SLi} - Y_{SL(i-1)}) R_L \tag{17}$$

where SLi is the soil layer i and SL(i-1) is the previous soil layer. The Y_{SLi} and $Y_{SL(i-1)}$ describe the cumulative proportion of roots from the surface to the soil layers i and i-1 accordingly. The vertical root distribution with depth (Y) is parametrized after Gale and Grigal (1987) as:

$$Y = 1 - \beta^d \tag{18}$$

where β describes the shape of the Y function and it is set to 0.953 (King et al., 2003) and d is the soil depth from surface (i.e. d = i*DZ, for i = [1,NSL]). The estimated root length density per soil layer is used for the calculation of the potentially extractable soil water and the total soil water uptake (Challinor et al., 2004). The value of the uptake diffusion coefficient (k_{DIF}) is taken from Jamieson and Ewert (1999).

3.5. Modelling the impact of water stress in GLAM-Parti

In GLAM the water stress factor describes the magnitude of water shortage - from full drought (value of zero), to zero water stress (value of one). For GLAM-Parti, the inverse number is used, so that the value of zero is appended to full water supply and this value increases according to the level of the water stress event. The soil water stress factor (SWFAC) is used to modify the SLA and the leaf:stem dry mass

allocation. These effects are modelled below.

3.5.1. Water stress effects on SLA

The function of canopy SLA is given in Section 3.4.1. In the absence of a robust relationship between the reduction of SLA and the magnitude of the water stress event, a linear relationship is assumed. The water stress effects on SLA are incorporated into Eq. (2) as following:

$$T_{mac} = \sum_{i=IEM}^{n} (1 + SWFAC) \cdot T_{max_i} \tag{19}$$

The incorporation of Eq. (19) into Eq. (1) results in a linear decrease of the canopy SLA according to the magnitude and the total period of the drought event.

3.5.2. Water stress effects on leaf:stem partitioning of biomass

In water limiting environments, the stem mass (M_S) is favoured over the leaf mass (M_L) for wheat (Ratjen et al., 2016). The enhancement of M_S is incorporated into GLAM-Parti as following:

$$M_{S_n} = h * \left(M_{L_{n-1}} + (1 + SWFAC) \cdot dM_L + M_{YL_n}\right)^g \tag{20}$$

where M_{S_n} and M_{YL_n} are the mass of stems and mass of yellow leaves on the n day, $M_{L_{n-1}}$ is the mass of green leaves on the previous day and dM_L is the leaf mass change between the two days. Eq. (20) can be used to describe Eq. (10) as:

$$M_{L_n} + M_{YL_n} + h * \left(M_{L_{n-1}} + (1 + SWFAC) \cdot dM_L + M_{YL_n}\right)^g - \frac{dW}{dt} - W_{n-1}$$
$$= 0 \tag{21}$$

and Eq. (21) can be described as a function of leaf area change (dL) as following:

$$\frac{LAI_{n-1} + dL}{SLA} + M_{YL_n} + h \cdot \left(\frac{LAI_{n-1} + (1 + SWFAC) \cdot dL}{SLA} + M_{YL_n}\right)^g - \frac{dW}{dt}$$
$$- W_{n-1} = 0 \tag{22}$$

Eq. (22) solves the system of equations for crop growth and development under water stress conditions. It is solved numerically with the Newton-Raphson method - similarly to Eq. (11) - to return the value of dL and calculate LAI as well as the masses of leaves, stems, and the total biomass under water stress. It consists of the second step of SEMAC, in which the water stress effects are incorporated into the model. The solution of Eq. (22) ensures consistency between the state variables and it outputs the attainable production level.

3.6. Sensitivity analysis to determine initial conditions for LAI

Eq. (11) does not converge for the first day after crop emergence, where the biomass of the previous day (W_{n-1}) equals zero. As a result, the solution of Eq. (11) does not return any real value of dL on that day. In order to solve this issue, an initial LAI value (LAI_{ini}) was prescribed into the model. LAI_{ini} consists of the initial condition of growth in GLAM-Parti and the model starts calculating the leaf area change from the second day after emergence. The baseline value of LAI_{ini} = 0.1365 m^2 m^{-2} was selected the model runs (Stella et al., 2014). The evolution of LAI is sensitive to LAI_{ini}, since every leaf area change depends on the LAI value of the previous time step. Analysis was conducted to evaluate the model performance over a wide range of LAI_{ini} values (interval (0.0007–0.3 m^2 m^{-2}), Ma et al., 2013). The model was calibrated for each LAI_{ini} using the methodology explained in Section 3.10.

3.7. Methods to compare sequential and simultaneous modelling methodologies

A new model version (GLAM-Parti$_{seq}$) was developed to test the contribution of the simultaneous equation modelling methodology to

the model output. The new version is identical to GLAM-Parti in terms of the model equations but it uses sequential method to solve them. In order to do this Eq. (11) was removed from the model. Instead, we use the LAI value of the previous time step (i.e. the previous day) to solve the model equations of the next day. The other model processes are not modified. Thus, the accumulation of biomass is estimated, which is partitioned into leaves and stems according to their allometric relationship. Given the mass of leaves and the canopy SLA, a new LAI is calculated, which is used for the solution of the model equations on the next day.

For a given set of equations there should be one set of parameters which optimizes the model output. GLAM-Parti and GLAM-Parti$_{seq}$ use the same set of equations but they differ in the model structure. As a result, one set of parameters is expected to lead to different model output in the two model versions. We made the assumption that GLAM-Parti provides higher internal consistency and that the parameters from the calibration of GLAM-Parti are the optimal for our set of model equations. If this is true, then GLAM-Parti should exhibit higher skill when the two model versions run with the parameters from its calibration. If not, then the assumption that GLAM-Parti improves the model performance due to the simultaneous modelling approach is wrong. Then we calibrated GLAM-Parti$_{seq}$, which resulted in new model output (i.e. we call it GLAM-Parti$_{seq-cal}$). If GLAM-Parti is still performing better than GLAM-Parti$_{seq-cal}$, this validates the assumption that the calibration of GLAM-Parti provides the optimal set of parameters for our set of model equations. The differences between GLAM-Parti and GLAM-Parti$_{seq}$ reveal the limitations of the sequential modelling approach. The comparison between GLAM-Parti and GLAM-Parti$_{seq-cal}$ shows the extend to which the calibration can compensate for the model limitations due to the step-wise modelling method.

3.8. Experimental design

GLAM, GLAM-Parti and GLAM-Parti$_{seq}$ were tested against field data for wheat under drought stress. The experiment, reported by Jamieson et al. (1995), was held in a mobile rainshelter at the New Zealand Institute for Crop and Food research experiment station at Lincoln in Canterbury (latitude 43˚38′ S, longitude 172˚30′ E). 'Batten' wheat was sown on 8 June 1991. The rainshelter was used to impose the plants to various levels of drought stress. Four treatments were chosen out of the total set of experiments for analysis here. Treatment 1 (RS1) is the control experiment which is well irrigated with no water stress, treatment 5 (RS5) is imposed to early drought, treatment 6 (RS6) is the late drought and treatment 11 (RS11) is the full drought experiment.

3.9. Statistical measures

The calibration and evaluation of all model versions was done using the root mean square error (RMSE) and model efficiency index (MEI) according to the following formulas:

$$RMSE = \sqrt{\frac{\sum_{n=1}^{n}(P_i - O_i)^2}{n}} \tag{23}$$

where P_i and O_i are the estimated and observed values accordingly and n equals the number of observations.

$$MEI = 1 - \frac{\sum_{n=1}^{n}(O_i - P_i)^2}{\sum_{n=1}^{n}(O_i - \bar{O})^2} \tag{24}$$

MEI is a measure of the model skill. It is in the range of $(-\infty, 1]$, where a value of 1 indicates ideal fit to the observations. Values below zero indicate that the mean observed value is a better predictor than the model (Krause et al., 2005).

3.10. Model calibration

GLAM, GLAM-Parti and GLAM-Parti$_{seq}$ were calibrated against the observed data. Initially, the simulated phenology of the models was set to meet the observed anthesis and maturity dates of the fully irrigated treatment. This was done to avoid any model bias from sources different than the water stress effects. The initial soil water and the soil characteristics were set up using the observed values. For transpiration efficiency (E_T) and maximum transpiration efficiency ($E_{TN,max}$), an optimizer was developed to test all possible combinations in their total range of values (see Appendix A for parameter ranges). The optimizer selected the combination of E_T and $E_{TN,max}$ which minimized the RMSE between all observed and simulated above-ground biomass values in the control experiment (RS1). For radiation use efficiency (RUE), the optimizer selected the value which minimized the RMSE between all observed and simulated above-ground biomass in the early drought treatment (RS5). This was done because RUE was used only after anthesis in the drought stress simulations (Section 3.1). Similar process was followed for the maximum LAI expansion rate $(dL/dt)_{max}$ and the rate of change of harvest index (dHI/dt). The optimizer selected the values which minimized the RMSE between observed and simulated LAI and grain mass of the control treatment (RS1) accordingly. The step for the runs of the optimizer was 0.1 for E_T, $E_{TN,max}$ and RUE, 0.0025 for $(dL/dt)_{max}$ and 0.00025 for dHI/dt. The $(dL/dt)_{max}$ parameter was used in all GLAM-Parti versions only for the period after anthesis when SEMAC stops and GLAM-Parti runs under the GLAM approach. The values of all calibrated parameters are provided in Table A.2 of Appendix A. The extinction coefficient k for wheat was set to 0.737 (Kanemasu et al., 1985) and the maximum transpiration rate (T_{Tmax}) was set to 0.75 cm day^{-1} (Liu et al., 2002). All other parameter values were taken from Challinor et al. (2004). The yield-gap parameter (C_{YG}) was set to one because limited water supply was the only yield-reducing factor.

4. Results

4.1. Test GLAM and GLAM-Parti overall model performance

Table 1 shows the MEI and RMSE of GLAM and GLAM-Parti for LAI, biomass, grain yield and cumulative evapotranspiration in all treatments. Both measures were calculated based on all simulated and observed values of the variables during the whole growing season. The mean MEI ($\overline{MEI}$) is the numerical mean of the four compared variables in each treatment.

Both models demonstrated a good agreement with the observations in the control experiment where no water stress effects the wheat (Fig. 7). The evapotranspiration, above-ground biomass and yield are well simulated in both models (i.e. all MEI values are greater or equal 0.94) and their overall performance is satisfactory. GLAM slightly overestimates the final yield, whilst GLAM-Parti overestimates the final biomass. Nevertheless, the differences are not large. GLAM is also in closer agreement with the maximum observed LAI value, whilst both models show very similar results in the simulation of the cumulative evapotranspiration. Overall, GLAM and GLAM-Parti show good performance in the simulation of the control treatment (GLAM $\overline{MEI}$ = 0.88, GLAM-Parti $\overline{MEI}$ = 0.92).

On the other hand, the performance of the two models varies considerably in the water stress treatments. In the early drought experiment (RS5), GLAM-Parti shows very good fit to the observations. In Fig. 8, both the leaf area development and the onset of leaf senescence are accurately estimated, whilst the peak LAI value is slightly underestimated. The simulated biomass and yield are also in close agreement with the observations (i.e. RMSE for biomass equals 0.69 and RMSE for yield equals 0.32), however the final yield is underestimated. On the contrary, GLAM shows lower skill in the simulation of RS5. The RMSE for LAI is higher in GLAM (1.30) than GLAM-Parti (0.45) and the

Table 1
Model efficiency index (MEI) and root mean square error (RMSE) of GLAM and GLAM-Parti for LAI (m^2 m^{-2}), Biomass (t ha^{-1}), Grain yield (t ha^{-1}) and Evapotranspiration (mm) in the four water treatments. RS1 is the control experiment, RS5 is early drought, RS6 is late drought and RS11 is the full drought experiment. $\overline{MEI}$ is the numerical mean of the four variables in each water treatment.

| Treatment	Model	LAI	Biomass	Grain yield	Evapotranspiration	$\overline{MEI}$
		MEI/RMSE	MEI/RMSE	MEI/RMSE	MEI/RMSE	
RS1	GLAM	0.59/1.69	0.94/1.97	0.99/0.26	0.99/22.31	0.88
RS5	GLAM	0.61/1.30	0.44/3.39	0.84/0.74	0.89/25.34	0.70
RS6	GLAM	0.40/1.78	0.71/2.89	0.94/0.49	0.84/36.03	0.72
RS11	GLAM	0.39/1.50	0.56/2.86	0.85/0.55	0.84/21.95	0.66
RS1	GLAM-Parti	0.74/1.34	0.95/1.81	1.00/0.23	0.99/23.19	0.92
RS5	GLAM-Parti	0.95/0.45	0.98/0.69	0.97/0.32	0.91/23.15	0.95
RS6	GLAM-Parti	0.80/1.00	0.97/0.99	0.98/0.29	0.82/38.76	0.89
RS11	GLAM-Parti	0.93/0.51	0.99/0.47	0.96/0.29	0.86/20.36	0.94
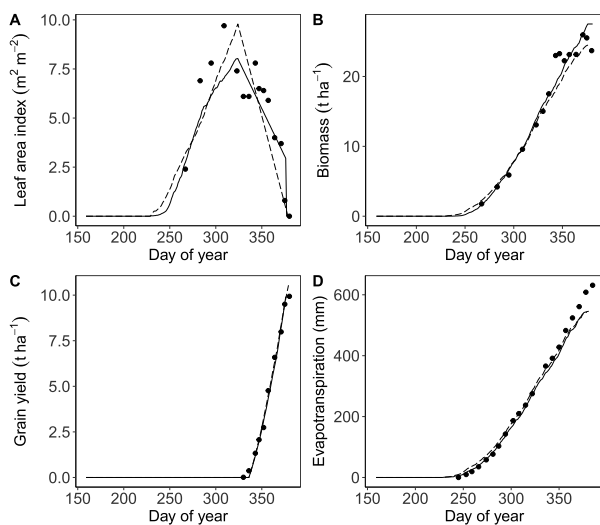
Fig. 7. Observed values (●), GLAM (− −) and GLAM-Parti (−) output in the control experiment (RS1) for: A. leaf area index (LAI), B. above-ground biomass, C. grain yield, D. cumulative evapotranspiration.
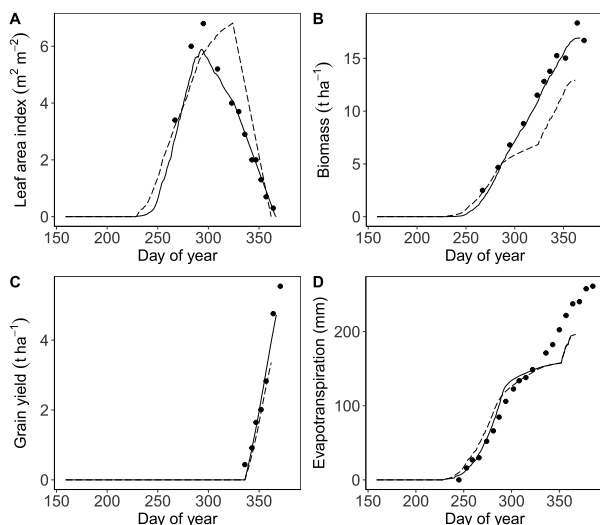

Fig. 8. Observed values (●), GLAM (− −) and GLAM-Parti (−) output in the early drought treatment (RS5) for: A. leaf area index (LAI), B. above-ground biomass, C. grain yield, D. cumulative evapotranspiration.

biomass is underestimated during almost the whole growing season. As a result, the grain growth and final yield are underestimated (Fig. 8). Regarding the evapotranspiration, both models show similar results.

Initially, they both overestimate the cumulative evapotranspiration and underestimate it later in the season. In summary, GLAM-Parti improves upon GLAM in the simulation of the early drought treatment (GLAM $\overline{MEI}$ = 0.70, GLAM-Parti $\overline{MEI}$ = 0.95).

In the late drought experiment (RS6), GLAM-Parti does not show an optimal agreement with the observations regarding the LAI development (RMSE = 1.00). In Fig. 9, the peak LAI value is slightly underestimated and the onset of LAI decline is delayed in comparison with the observations. This is due to the initiation of the water stress effects in the model later than the reality. In addition, the LAI decline rate is underestimated after anthesis. As a result, the model simulates an increased number of grain filling days, which leads to a significant overestimation of the final grain yield. Nevertheless, the above-ground biomass is well estimated (i.e. RMSE = 0.99). On the other hand, GLAM shows lower performance in the simulation of LAI in the RS6 treatment (RMSE = 1.78). The above-ground biomass is underestimated and this leads to an underestimation of the final yield. Moreover, both models show similar results in the simulation of evapotranspiration. They are in good agreement with the observations apart from the last period of the crop cycle when it is underestimated. Overall, GLAM-Parti improves over GLAM in the simulation of the RS6 treatment (GLAM $\overline{MEI}$ = 0.89, GLAM-Parti $\overline{MEI}$ = 0.72).

In the full drought experiment (RS11), the leaf growth and senescence rate are accurately simulated in GLAM-Parti (Fig. 10) and the LAI is well estimated (RMSE = 0.51). Similarly, the model shows a very good fit to the observed biomass (RMSE = 0.47), whilst the final yield
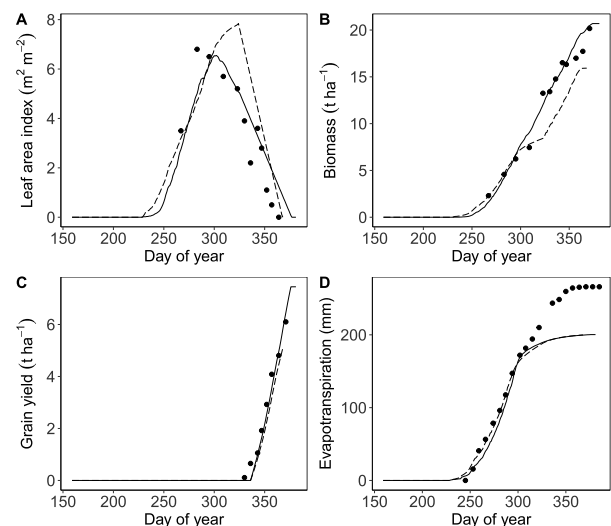

Fig. 9. Observed values (●), GLAM (− −) and GLAM-Parti (−) output in the late drought experiment (RS6) for: A. leaf area index (LAI), B. above-ground biomass, C. grain yield, D. cumulative evapotranspiration.
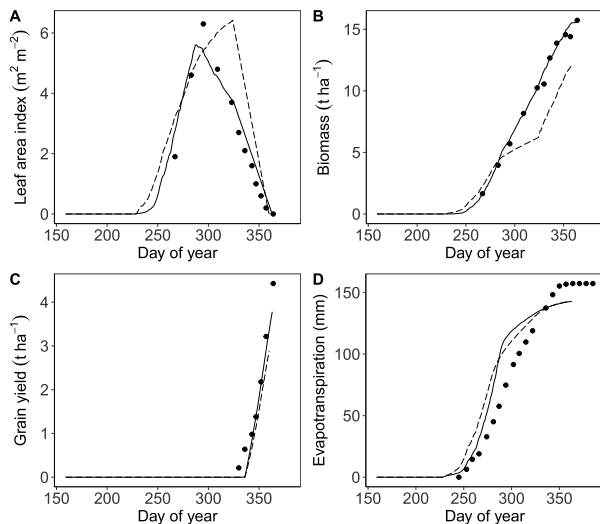
Fig. 10. Observed values (●), GLAM (– –) and GLAM-Parti (–) output in the full drought experiment (RS11) for: A. leaf area index (LAI), B. above-ground biomass, C. grain yield, D. cumulative evapotranspiration.

is slightly underestimated (RMSE = 0.29). On the contrary, GLAM shows a lower performance in the simulation of leaf growth and senescence and the estimation of LAI (RMSE = 1.50). The above-ground biomass is underestimated during almost the whole crop season, as well as the grain yield. The cumulative evapotranspiration shows similar pattern in both models, by being overestimated during the most part of the growing season and underestimated in the final part. In summary, GLAM-Parti advantages over GLAM in the simulation of the full drought treatment (GLAM $\overline{MEI}$ = 0.66, GLAM-Parti $\overline{MEI}$ = 0.94).

4.2. Results of sensitivity analysis

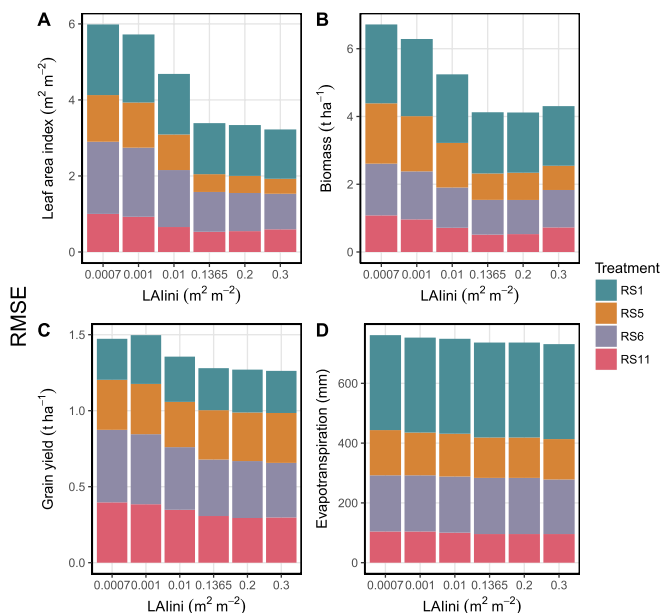Fig. 11 shows the RMSE for LAI, biomass, grain yield and

Fig. 11. Barplots of the root mean square error (RMSE) between modelled (GLAM-Parti) and observed state variables: A. leaf area index (LAI), B. above-ground biomass, C. grain yield, D. cumulative evapotranspiration in the different water treatments: Control treatment (RS1), early drought treatment (RS5), late drought treatment (RS6), full drought treatment (RS11).
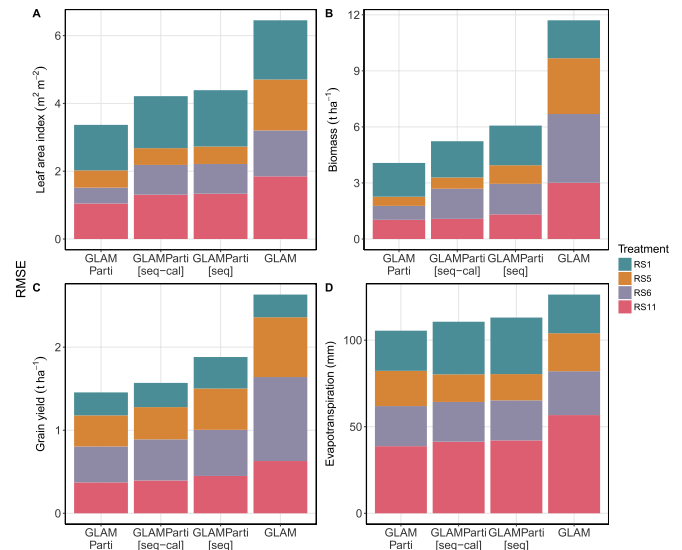

Fig. 12. Barplots of the root mean square error (RMSE) between modelled and observed state variables: A. leaf area index (LAI), B. above-ground biomass, C. grain yield, D. cumulative evapotranspiration in the different water treatments: Control treatment (RS1), early drought treatment (RS5), late drought treatment (RS6), full drought treatment (RS11). The four models under comparison are: GLAM, GLAM-Parti, GLAM-Parti$_{seq}$ and GLAM-Parti$_{seq-cal}$.

evapotranspiration in the total range of LAI$_{ini}$ in GLAM-Parti. For all compared variables, the lowest RMSE was achieved in the [0.1365–0.3] range. For the LAI$_{ini}$ values in the low range ([0.0007–0.01]), the model showed a consistently higher RMSE for all variables, especially for LAI and biomass. The total RMSE was at least 27.5% higher for LAI, 17.9% higher for biomass, 5.6% higher for grain yield and 1.7% higher for evapotranspiration in the low LAI$_{ini}$ range. This further supports the use of a LAI$_{ini}$ value in the [0.1365–0.3] range for the model runs. Furthermore, Fig. 11 shows that the model calibration does not compensate for the variability in LAI$_{ini}$ at the low range ([0.0007–0.01]). Hence, in GLAM-Parti, attention should be given to the parameterization of LAI$_{ini}$, since the model can be sensitive to its value.

4.3. Comparison of simultaneous and sequential modelling approaches

GLAM, GLAM-Parti, GLAM-Parti$_{seq}$ and GLAM-Parti$_{seq-cal}$ were compared against the observations for LAI, biomass, grain yield and evapotranspiration in the four water treatments. The RMSE was used to measure the model skill and it was calculated based on all observed and simulated values of each variable during the growing season. Fig. 12 shows that GLAM exhibits higher total RMSE in all treatments than any GLAM-Parti version by at least 46.9% for LAI, 92.9% for biomass, 39.9% for grain yield and 11.7% for evapotranspiration (Fig. 12). This reveals that the model modifications lead to significant improvement in the overall performance regardless of the modelling methodology implemented (i.e. sequential or simultaneous). Next, the impact of the model structure was tested by comparing GLAM-Parti with GLAM-Parti$_{seq}$. The total RMSE of GLAM-Parti$_{seq}$ was higher than GLAM-Parti as following: 30.4% for LAI, 49.1% for biomass, 29.3% for yield and 7.2% for evapotranspiration. Similarly, the total RMSE of GLAM-Parti$_{seq-cal}$ was higher than GLAM-Parti by 25.2% for LAI, 28.6% for biomass, 7.9% for yield and 4.9% for evapotranspiration. The above results highlight the need of solving the model equations simultaneously to overcome the structural limitations of the sequential modelling approach. In all comparisons of this study, GLAM-Parti improves upon any model version. The calibration can only partially but not fully compensate for the inconsistencies of the sequential method. Therefore, our results indicate that the incorporation of SEMAC increases the

model skill both due to the model modifications and the simultaneous modelling methodology.

5. Discussion

The incorporation of SEMAC into GLAM leads to a significant model improvement in the four rain-shelter experiments. The major differences between the two model versions rely on the simulation of the leaf dynamics, the partitioning of dry matter to the plant compartments and the model structure. The structure of GLAM requires the use of the water stress factor on the reduction of LAI growth under drought. On the contrary, GLAM-PARTI removes the stress effects from LAI. This is crucial for the model ability to simulate the observed leaf dynamics and the overall plant growth. In the experiments, under water stress there is premature leaf senescence which leads to an earlier LAI decline. This effect cannot be captured in GLAM with the use of the water stress factor acting on LAI. The SWFAC takes only positive values (from zero to one), and when applied to the leaf area change, it leads to an increased trend of LAI growth (even though at a reduced rate) instead of the observed decline. This opposite leaf area trend gives a significant error in GLAM and it contributes to the limited model skill in capturing the water stress effects.

On the other hand, the SEMAC methodology is seen to be successful in the prediction of the leaf dynamics. The canopy SLA varies during the season and this affects both the already formed leaf tissue and the newly formed leaf area (i.e. in Eq. (11) the SLA acts both on the already existing LAI and the newly formed leaf area (dL)). Thus, the SLA of the previously formed leaf tissue is not conserved (Ratjen and Kage, 2013). The water stress factor is removed from LAI and the model error is reduced. In GLAM-Parti, the LAI value is extracted by the system of equations after incorporating the water stress effects. This technique explicitly takes into account the drought-induced changes on leaf growth and development and enables the prediction of the acceleration of leaf senescence without further parameterization. Fig. 13 shows the simulated LAI of all treatments until the day of anthesis, when SEMAC stops. It can be seen that the LAI curve of all drought treatments declines earlier than the control. The maximum LAI value is lower in all water stress treatments, and the LAI profile is altered, with early senescence affecting the wheat. The improved simulation of leaf senescence is due to the SEMAC methodology which introduces

Fig. 13. Simulated LAI of all treatments until day of anthesis in GLAM-Parti. Control treatment (RS1) (continuous line), early drought (RS5) (twodash line), late drought (RS6) (dashed line), full drought (RS11) (dotted line).

modifications to the leaf dynamics and the partitioning of dry matter and it extracts the leaf area change from the system of equations. Thus, the leaf area change is not restricted only to positive values during the pre - senescence stage (i.e. as in GLAM with the use of the SWFAC on LAI), but it can also be negative during any part of the crop cycle – depending on the existence and the magnitude of the stress event. As a result, GLAM-Parti successfully captures the premature leaf senescence without the need of downscaling into leaf level processes. This is an important trait of SEMAC and it can be used as a significant tool in the attempt to model the plant performance in various stress environments. It is also a key aspect for the improved simulation of the drought effects in this study. The same modifications could not be implemented in the original GLAM model where LAI and biomass are not jointly determined. Hence, the inclusion of SEMAC improves the estimation of the water stress effects on wheat.

SEMAC provides a robust model structure which leads to a more realistic representation of crop growth and development as well as an improved simulation of the water stress effects. Moreover, the methodology follows the general remark that an improvement in the simulation of the leaf dynamics is essential for the further development of crop models (Ewert, 2004). This is especially true under stress conditions where modelling of leaf development becomes more complex and it can lead to systematic errors. For instance, it has already been seen that in modelling of heat stress, the omission of the acceleration of leaf senescence for wheat increases the model error significantly (Maiorano et al., 2017). Here, the capture of premature leaf senescence under drought in GLAM-Parti significantly improves the model performance.

The contribution of the simultaneous solution of the model equations to the model performance was separated from the model modifications. For this reason, GLAM-Parti was re-designed to solve the model equations sequentially (GLAM-Parti$_{seq}$). The comparison of GLAM-Parti and GLAM-Parti$_{seq}$ highlights the limitations of the sequential modelling approach. GLAM-Parti$_{seq}$ shows higher RMSE than GLAM-Parti in all compared variables. This reveals that the inconsistencies introduced by the sequential solution of equations affect the model skill. GLAM-Parti$_{seq-cal}$ improves the model performance but it does not fully compensate for the inconsistencies of the sequential approach. As a result, GLAM-Parti$_{seq-cal}$ has higher RMSE than GLAM-Parti for all compared variables. Thus, the simultaneous equation modelling leads to significant model improvement due to the robustness of the model structure.

SEMAC can be implemented in other transpiration or radiation use efficiency models with a similar methodology to the one presented here. Initially, allometric relationships should be introduced to partition the biomass (W_n) to the different plant compartments. This gives the opportunity to express W_n as function of LAI. The accumulation of new biomass (dW/dt) can also be expressed as function of LAI. For transpiration driven models, this can be done using an approach similar to the one presented here. In radiation use efficiency models, dW/dt can be expressed as function of LAI as shown in Fig. 2. The expression of W_n and dW/dt as function of LAI develops an equation similar to Eq. (11) which is solved to return the LAI value. This is done twice, initially for optimal environmental conditions, where the impact of stresses is ignored and then again after incorporating the stress effects. LAI is then used to calculate all variables in the system of equations. Regarding the stress effects, these can be simulated by reducing the accumulation of new biomass, altering the carbon allocation between the plant parts and adjusting the canopy SLA. Various models use different techniques to simulate these modifications. The model performance will depend on the efficiency to capture the above-mentioned effects at the canopy level. More effort may be needed to implement SEMAC in more detailed crop models (i.e. photosynthesis based models), where the model complexity may increase the difficulty of solving the system of equations simultaneously. Currently, there is no clear path on how to incorporate SEMAC in these models. Thus, the approach is mainly aimed
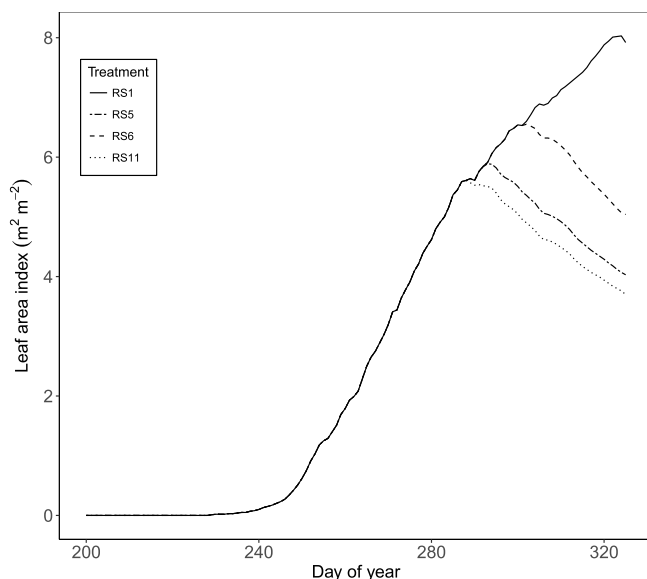
to radiation or transpiration based models of medium complexity like GLAM. However, the possibility of implementing SEMAC in more complex models is not excluded, but simplifications in the model structure may be needed.

Finally, in the late drought treatment GLAM-Parti overestimates the final yield. This is due to the increased number of grain filling days in the model simulation. Currently SEMAC stops at anthesis and during that period GLAM-Parti runs under the GLAM approach. Thus, SEMAC needs to be expanded for the period after anthesis. In addition, the modelling of yellow leaf mass should be improved, since Eq. (12) is currently not included into the system of equations.

6. Conclusion

The application of SEMAC to crop modelling results in a new model where all equations for crop growth and development are combined and solved simultaneously. It is adopted here into the GLAM crop model and a new model version is formed (GLAM-Parti). The new model is primarily designed to deal with stress conditions, where various processes are modified and modelling the plant performance becomes more difficult.

The incorporation of SEMAC into GLAM simplifies the model algorithms and improves upon the simulation of several plant processes (e.g. LAI development, acceleration of leaf senescence under water stress conditions, leaf:stem partitioning of biomass). These alterations lead to an improved model performance and a more realistic model output. We demonstrated this by testing the two model versions against different levels of water stress. GLAM-Parti showed a clear improvement over GLAM in all drought simulations. In addition, GLAM-Parti retains its confidence at all levels of water stress in the treatments (i.e. from early to full drought treatment).

In general, we believe that a robust model structure is essential for the realistic simulation of crop performance under stress conditions. The success of SEMAC relies on the improved model structure, the better representation of the leaf dynamics and the improved internal model consistency. SEMAC can be further extended to incorporate more

stresses. Application of SEMAC to other crop models would follow a similar methodology to that presented here. It would be very interesting to see if similar improvements in skill result. Finally, it is believed that SEMAC can be a useful tool for the simulation of the crop performance under climate variability and change where multiple stresses may act on crops simultaneously.

Software and data availability

Acknowledgements

Appendix A

The equations of potential evapotranspiration ($E_{pot}T$), potential transpiration (T_T) and biomass growth (dW/dt) are taken from Challinor et al. (2004).

Potential evapotranspiration:

$$E_{pot}^T = \frac{\alpha}{\lambda} \cdot \frac{\Delta(R_N - G)}{\Delta + \gamma}$$

$$= \frac{\alpha}{\lambda} \cdot \frac{\Delta(R_N - C_G \cdot R_N \cdot e^{-kLAI})}{\Delta + \gamma}$$

$$= \frac{\alpha \cdot \Delta \cdot R_N}{\lambda \cdot (\Delta + \gamma)} \cdot (1 - C_G e^{-kLAI}) \tag{A.1}$$

Eq. (A.1) can be used to express potential transpiration as:

$$T_T = E_{pot}^T \cdot (1 - e^{-kLAI})$$

$$= \frac{\alpha \cdot \Delta \cdot R_N}{\lambda \cdot (\Delta + \gamma)} \cdot (1 - C_G \cdot e^{-kLAI})(1 - e^{-kLAI}) \tag{A.2}$$

Eq. (A.2) can be used to describe biomass growth (dW/dt) as:

$$\frac{dW}{dt} = TE \cdot T_T$$

$$= TE \cdot \frac{\alpha \cdot \Delta \cdot R_N}{\lambda \cdot (\Delta + \gamma)} \cdot (1 - C_G \cdot e^{-kLAI}) \cdot (1 - e^{-kLAI}) \tag{A.3}$$

Eq. (A.3) consists of the dW/dt term in Eq. (11). The C_G, k, γ and λ are constants and the α, Δ, R_N, TE are dependent on the environmental conditions. After calculating the environmental dependence, the dW/dt becomes a function of LAI. Detailed description of all parameters and equations is provided in Challinor et al. (2004).

Table A.2

Values and units of calibrated parameters for GLAM, GLAM-Parti and GLAM-Parti$_{seq}$.

Parameter	Unit	Range	GLAM value	GLAM-Parti value	GLAM-Parti$_{seq}$ value	Source
E_T	Pa	[3.5–6]	3.5	3.5	3.5	Sanai et al. (2010)
$E_{TN,max}$	g kg^{-1}	[5–9]	5	5.6	5.8	Sanai et al. (2010)
Post – anthesis RUE	g MJ^{-1} PAR	[1.2–2.0]	2.0	2.0	2.0	Calderini et al. (1997)
$(dL/dt)_{max}$	m^2 m^{-2} d^{-1}	[0.06–0.28]	0.18	0.09 [a]	0.095 [a]	Sanai et al. (2010), Jamieson et al. (1995)
dHI/dt	d^{-1}	[0.0064–0.0137]	0.01	0.009	0.009	Moot et al. (1996)

[a] $(dL/dt)_{max}$ is used only after anthesis when SEMAC stops and the model runs under the GLAM approach.

References

Affholder, F., Tittonell, P., Corbeels, M., Roux, S., Motisi, N., Tixier, P., Wery, J., 2012. Ad hoc modeling in agronomy: what have we learned in the last 15 years? Agron. J. 104 (3), 735–748.

Asseng, S., Ewert, F., Martre, P., Rötter, R.P., Lobell, D., Cammarano, D., Kimball, B., Ottman, M., Wall, G., White, J.W., et al., 2015. Rising temperatures reduce global wheat production. Nat. Clim. Change 5 (2), 143.

Asseng, S., Ewert, F., Rosenzweig, C., Jones, J., Hatfield, J., Ruane, A., Boote, K.J., Thorburn, P.J., Rötter, R.P., Cammarano, D., et al., 2013. Uncertainty in simulating wheat yields under climate change. Nat. Clim. Change 3 (9), 827.

Asseng, S., Jamieson, P., Kimball, B., Pinter, P., Sayre, K., Bowden, J., Howden, S., 2004. Simulated wheat growth affected by rising temperature, increased water deficit and elevated atmospheric co2. Field Crop. Res. 85 (2–3), 85–102.

Asseng, S., Turner, N.C., Botwright, T., Condon, A.G., 2003. Evaluating the impact of a trait for increased specific leaf area on wheat yields using a crop simulation model. Agron. J. 95 (1), 10–19.

Atkin, O.K., Loveys, B., Atkinson, L.J., Pons, T., 2005. Phenotypic plasticity and growth temperature: understanding interspecific variability. J. Exp. Bot. 57 (2), 267–281.

Baldocchi, D., 1994. An analytical solution for coupled leaf photosynthesis and stomatal conductance models. Tree Physiol. 14 (7–8–9), 1069–1079.

Baret, F., Olioso, A., Luciani, J., 1992. Root biomass fraction as a function of growth degree days in wheat. Plant Soil 140 (1), 137–144.

Brisson, N., Casals, M.-L., 2005. Leaf dynamics and crop water status throughout the growing cycle of durum wheat crops grown in two contrasted water budget conditions. Agron. Sustain. Dev. 25 (1), 151–158.

Calderini, D.F., Dreccer, M.F., Slafer, G.A., 1997. Consequences of breeding on biomass, radiation interception and radiation-use efficiency in wheat. Field Crop. Res. 52 (3), 271–281.

Challinor, A., Slingo, J., Wheeler, T., Doblas-Reyes, F., 2005. Probabilistic simulations of crop yield over western India using the demeter seasonal hindcast ensembles. Tellus 57 (3), 498–512.

Challinor, A., Wheeler, T., Craufurd, P., Slingo, J., Grimes, D., 2004. Design and optimisation of a large-area process-based model for annual crops. Agric. For. Meteorol. 124 (1–2), 99–120.

Challinor, A.J., Ewert, F., Arnold, S., Simelton, E., Fraser, E., 2009. Crops and climate change: progress, trends, and challenges in simulating impacts and informing adaptation. J. Exp. Bot. 60 (10), 2775–2789.

Challinor, A.J., Müller, C., Asseng, S., Deva, C., Nicklin, K.J., Wallach, D., Vanuytrecht, E., Whitfield, S., Ramirez-Villegas, J., Koehler, A.-K., 2018. Improving the use of crop models for risk assessment and climate change adaptation. Agric. Syst. 159, 296–306.

Challinor, A.J., Smith, M.S., Thornton, P., 2013. Use of agro-climate ensembles for quantifying uncertainty and informing adaptation. Agric. For. Meteorol. 170, 2–7.

Challinor, A.J., Watson, J., Lobell, D., Howden, S., Smith, D., Chhetri, N., 2014. A meta-analysis of crop yield under climate change and adaptation. Nat. Clim. Change 4 (4), 287.

Chenu, K., Porter, J.R., Martre, P., Basso, B., Chapman, S.C., Ewert, F., Bindi, M., Asseng, S., 2017. Contribution of crop models to adaptation in wheat. Trends Plant Sci. 22 (6), 472–490.

Chou, J.C., Kamel, M., 1988. Quaternions approach to solve the kinematic equation of rotation, a/sub a a/sub x/= a/sub x a/sub b/, of a sensor-mounted robotic manipulator. In: Robotics and Automation, 1988. Proceedings., 1988 IEEE International Conference on. IEEE, pp. 656–662.

Cramer, G.R., Urano, K., Delrot, S., Pezzotti, M., Shinozaki, K., 2011. Effects of abiotic stress on plants: a systems biology perspective. BMC Plant Biol. 11 (1), 163.

Enquist, B.J., Brown, J.H., West, G.B., 1998. Allometric scaling of plant energetics and population density. Nature 395 (6698), 163.

Ewert, F., 2004. Modelling plant responses to elevated co2: how important is leaf area index? Ann. Bot. 93 (6), 619–627.

Ewert, F., Rötter, R.P., Bindi, M., Webber, H., Trnka, M., Kersebaum, K.C., Olesen, J.E., van Ittersum, M.K., Janssen, S., Rivington, M., et al., 2015. Crop modelling for integrated assessment of risk to food production from climate change. Environ. Model. Softw 72, 287–303.

Fernández, R.J., Reynolds, J.F., 2000. Potential growth and drought tolerance of eight desert grasses: lack of a trade-off? Oecologia 123 (1), 90–98.

Gale, M., Grigal, D., 1987. Vertical root distributions of northern tree species in relation to successional status. Can. J. For. Res. 17 (8), 829–834.

Goudriaan, J., Van Laar, H., 1994. Modelling Potential Crop Growth Processes: Textbook with Exercises, vol. 2 Springer Science & Business Media.

Gray, S.B., Brady, S.M., 2016. Plant developmental responses to climate change. Dev. Biol. 419 (1), 64–77.

Hoogenboom, G., Jones, J., Boote, K., 1992. Modeling growth, development, and yield of grain legumes using soygro, pnutgro, and beangro: a review. Trans. ASAE 35 (6), 2043–2056.

Hotsonyame, G., Hunt, L., 1998. Seeding date, photoperiod and nitrogen effects on specific leaf area of field-grown wheat. Can. J. Plant Sci. 78 (1), 51–61.

Howden, S.M., Soussana, J.-F., Tubiello, F.N., Chhetri, N., Dunlop, M., Meinke, H., 2007. Adapting agriculture to climate change. Proc. Natl. Acad. Sci. Unit. States Am. 104 (50), 19691–19696.

Inoue, T., Inanaga, S., Sugimoto, Y., El Siddig, K., 2004. Contribution of pre-anthesis assimilates and current photosynthesis to grain yield, and their relationships to drought resistance in wheat cultivars grown under different soil moisture. Photosynthetica 42 (1), 99–104.

Jamieson, P., Ewert, F., 1999. The role of roots in controlling soil water extraction during drought: an analysis by simulation. Field Crop. Res. 60 (3), 267–280.

Jamieson, P., Martin, R., Francis, G., 1995. Drought influences on grain yield of barley, wheat, and maize. N. Z. J. Crop Hortic. Sci. 23 (1), 55–66.

Jamieson, P., Porter, J., Goudriaan, J., Ritchie, J. v., Van Keulen, H., Stol, W., 1998. A comparison of the models afrcwheat2, ceres-wheat, sirius, sucros2 and swheat with measurements from wheat grown under drought. Field Crop. Res. 55 (1–2), 23–44.

Jones, G.D., Droz, B., Greve, P., Gottschalk, P., Poffet, D., McGrath, S.P., Seneviratne, S.I., Smith, P., Winkel, L.H., 2017. Selenium deficiency risk predicted to increase under future climate change. In: Proceedings of the National Academy of Sciences, 201611576.

Kanemasu, E., Asrar, G., Fuchs, M., 1985. Application of remotely sensed data in wheat growth modelling. In: Wheat Growth and Modelling. Springer, pp. 357–369.

King, J., Gay, A., Sylvester-Bradley, R., Bingham, I., Foulkes, J., Gregory, P., Robinson, D., 2003. Modelling cereal root systems for water and nitrogen capture: towards an economic optimum. Ann. Bot. 91 (3), 383–390.

Krause, P., Boyle, D., Bäse, F., 2005. Comparison of different efficiency criteria for hydrological model assessment. Adv. Geosci. 5, 89–97.

Lefcheck, J.S., 2016. piecewisesem: piecewise structural equation modelling in r for ecology, evolution, and systematics. Meth. Ecol. Evol. 7 (5), 573–579.

Leutscher, K., Vogelezang, J., 1990. A crop growth simulation model for operational management support in pot plant production. Agric. Syst. 33 (2), 101–114.

Liu, C., Zhang, X., Zhang, Y., 2002. Determination of daily evaporation and evapotranspiration of winter wheat and maize by large-scale weighing lysimeter and microlysimeter. Agric. For. Meteorol. 111 (2), 109–120.

Loomis, R.S., Rabbinge, R., Ng, E., 1979. Explanatory models in crop physiology. Annu. Rev. Plant Physiol. 30 (1), 339–367.

Loveys, B., Scheurwater, I., Pons, T., Fitter, A., Atkin, O., 2002. Growth temperature influences the underlying components of relative growth rate: an investigation using inherently fast-and slow-growing plant species. Plant Cell Environ. 25 (8), 975–988.

Ma, G., Huang, J., Wu, W., Fan, J., Zou, J., Wu, S., 2013. Assimilation of modis-lai into the wofost model for forecasting regional winter wheat yield. Math. Comput. Model. 58 (3–4), 634–643.

Mahrookashani, A., Siebert, S., Hüging, H., Ewert, F., 2017. Independent and combined effects of high temperature and drought stress around anthesis on wheat. J. Agron. Crop Sci. 203 (6), 453–463.

Maiorano, A., Martre, P., Asseng, S., Ewert, F., Müller, C., Rötter, R.P., Ruane, A.C., Semenov, M.A., Wallach, D., Wang, E., et al., 2017. Crop model improvement reduces the uncertainty of the response to temperature of multi-model ensembles. Field Crop. Res. 202, 5–20.

Marcelis, L., Heuvelink, E., 2007. Concepts of modelling carbon allocation among plant organs. Frontis 103–111.

Marcelis, L., Heuvelink, E., Goudriaan, J., 1998. Modelling biomass production and yield of horticultural crops: a review. Sci. Hortic. 74 (1–2), 83–111.

Martre, P., Kimball, B.A., Ottman, M.J., Wall, G.W., White, J.W., Asseng, S., Ewert, F., Cammarano, D., Maiorano, A., Aggarwal, P.K., et al., 2018. The hot serial cereal experiment for modeling wheat response to temperature: field experiments and agmip-wheat multi-model simulations. Open Data J. Agric. Res. 4, 28–34.

Mittler, R., 2006. Abiotic stress, the field environment and stress combination. Trends Plant Sci. 11 (1), 15–19.

Moot, D., Jamieson, P., Henderson, A., Ford, M., Porter, J., 1996. Rate of change in harvest index during grain-filling of wheat. J. Agric. Sci. 126 (4), 387–395.

Myers, S.S., Zanobetti, A., Kloog, I., Huybers, P., Leakey, A.D., Bloom, A.J., Carlisle, E., Dietterich, L.H., Fitzgerald, G., Hasegawa, T., et al., 2014. Increasing co 2 threatens human nutrition. Nature 510 (7503), 139.

Oldroyd, J., 1950. On the formulation of rheological equations of state. Proc. Roy. Soc.

Lond. A 200 (1063), 523–541.

Osborne, T., Rose, G., Wheeler, T., 2013. Variation in the global-scale impacts of climate change on crop productivity due to climate model uncertainty and adaptation. Agric. For. Meteorol. 170, 183–194.

Passioura, J.B., 1996. Simulation models: science, snake oil, education, or engineering? Agron. J. 88 (5), 690–694.

Poorter, H., Niklas, K.J., Reich, P.B., Oleksyn, J., Poot, P., Mommer, L., 2012. Biomass allocation to leaves, stems and roots: meta-analyses of interspecific variation and environmental control. New Phytol. 193 (1), 30–50.

Porter, J.R., Xie, L., Challinor, A.J., Cochrane, K., Howden, S.M., Iqbal, M.M., Lobell, D.B., Travasso, M.I., Netra Chhetri, N.C., Garrett, K., et al., 2014. Food Security and Food Production Systems.

Raes, D., Steduto, P., Hsiao, T.C., Fereres, E., 2009. Aquacrop—the fao crop model to simulate yield response to water: ii. main algorithms and software description. Agron. J. 101 (3), 438–447.

Ramirez-Villegas, J., Koehler, A.-K., Challinor, A.J., 2017. Assessing uncertainty and complexity in regional-scale crop model simulations. Eur. J. Agron. 88, 84–95.

Ratjen, A., Neukam, D., Kage, H., 2016. A simple drought-sensitive model for leaf: stem partitioning of wheat. J. Agron. Crop Sci. 202 (4), 300–308.

Ratjen, A.M., Kage, H., 2013. Is mutual shading a decisive factor for differences in overall canopy specific leaf area of winter wheat crops? Field Crop. Res. 149, 338–346.

Rivington, M., Koo, J., 2010. Report on the Meta-Analysis of Crop Modelling for Climate Change and Food Security Survey.

Rosbakh, S., Römermann, C., Poschlod, P., 2015. Specific leaf area correlates with temperature: new evidence of trait variation at the population, species and community levels. Alpine Bot. 125 (2), 79–86.

Sanai, L., Wheeler, T., Challinor, A., Erda, L., Yinlong, X., Hui, J., 2010. Simulating the impacts of global warming on wheat in China using a large area crop model. J Meteorol Res 24 (1), 123–135.

Sieling, K., Böttcher, U., Kage, H., 2016. Dry matter partitioning and canopy traits in wheat and barley under varying n supply. Eur. J. Agron. 74, 1–8.

Sinclair, T.R., Seligman, N., 2000. Criteria for publishing papers on crop modeling. Field Crop. Res. 68 (3), 165–172.

Stella, T., Frasso, N., Negrini, G., Bregaglio, S., Cappelli, G., Acutis, M., Confalonieri, R., 2014. Model simplification and development via reuse, sensitivity analysis and composition: a case study in crop modelling. Environ. Model. Softw 59, 44–58.

Tao, F., Rötter, R.P., Palosuo, T., Gregorio Hernández Díaz-Ambrona, C., Mínguez, M.I., Semenov, M.A., Kersebaum, K.C., Nendel, C., Specka, X., Hoffmann, H., et al., 2018. Contribution of crop model structure, parameters and climate projections to uncertainty in climate change impact assessments. Glob. Chang. Biol. 24 (3), 1291–1307.

Taylor, S., Payton, M., Raun, W., 1999. Relationship between mean yield, coefficient of variation, mean square error, and plot size in wheat field experiments. Commun. Soil Sci. Plant Anal. 30 (9–10), 1439–1447.

Van Ittersum, M., Rabbinge, R., 1997. Concepts in production ecology for analysis and quantification of agricultural input-output combinations. Field Crop. Res. 52 (3), 197–208.

van Ittersum, M.K., Leffelaar, P.A., Van Keulen, H., Kropff, M.J., Bastiaans, L., Goudriaan, J., 2003. On approaches and applications of the wageningen crop models. Eur. J. Agron. 18 (3–4), 201–234.

Weiner, J., 2004. Allocation, plasticity and allometry in plants. Perspect. Plant Ecol. Evol. Systemat. 6 (4), 207–215.

Yin, X., Struik, P., 2009. C3 and c4 photosynthesis models: an overview from the perspective of crop modelling. NJAS - Wageningen J. Life Sci. 57 (1), 27–38.

Yin, X., Struik, P.C., 2010. Modelling the crop: from system dynamics to systems biology. J. Exp. Bot. 61 (8), 2171–2183.

Zeng, D., Cai, J., 2005. Simultaneous modelling of survival and longitudinal data with an application to repeated quality of life measures. Lifetime Data Anal. 11, 151–174.

Zhang, B., Liu, W., Chang, S.X., Anyia, A.O., 2010. Water-deficit and high temperature affected water use efficiency and arabinoxylan concentration in spring wheat. J. Cereal Sci. 52 (2), 263–269.

Zhang, S., Tao, F., 2013. Modeling the response of rice phenology to climate change and variability in different climatic zones: comparisons of five models. Eur. J. Agron. 45, 165–176.

Zhao, C., Liu, B., Piao, S., Wang, X., Lobell, D.B., Huang, Y., Huang, M., Yao, Y., Bassu, S., Ciais, P., et al., 2017. Temperature increase reduces global yields of major crops in four independent estimates. Proc. Natl. Acad. Sci. Unit. States Am. 114 (35), 9326–9331.